

Falla de talud en la costa del Paraná, Argentina

Slope failure at the Paraná shoreline, Argentina

Alejo O. Sfriso

UBA and Verri&Sfriso, member ASCE.

Juan Larrague

UBA and Larrague y Asociados, member ASCE.

Resumen

En la margen derecha del Paraná de las Palmas se construyó un terraplén de 80000 m² y 3.5 m de altura para una playa de contenedores. Sobre él se colocó un terraplén temporario de 3.5 m de altura para acelerar el proceso de consolidación de las arcillas blandas y suelos orgánicos subyacentes. La construcción del terraplén de precarga tomó aproximadamente cuatro meses. La precarga fue demorada en una pequeña superficie de 6000 m² debido a actividades de operación portuaria. Varios meses más tarde y utilizando los mismos equipos, el contratista completó el terraplén de precarga de esta pequeña área en diez días. Un día luego de completada la precarga se produjo una falla masiva de talud. Presentamos los resultados del análisis de esta falla de talud, las medidas de remediación adoptadas y algunos comentarios acerca del comportamiento de los suelos de la costa del Paraná.

Abstract

A 80000 m², 3.5 m high embankment for a container yard was constructed on the right margin of the Paraná de las Palmas River in Zárate, Argentina. An additional temporary embankment, 3.5 m high, was put on top of it to speed up the consolidation process of underlying soft Postpampeano clays and organic soils. The construction of the preload embankment took about four months. The preload was delayed in a small area of 6000 m² because of harbour activities. Several months later, and using the same equipment, the contractor completed the preload embankment of this small area within ten days. One day after completion of the preload, a massive slope failure occurred. In this paper, the results of the analyses of the slope failure, the remediation action undertaken and some comments on the behavior of the soils at the Paraná shoreline are presented.

1 INTRODUCTION

A container terminal project was constructed on the right margin of Paraná de las Palmas River, in Zárate, 90 km north of Buenos Aires, Argentina. Works included the extension of an existing wharf, the construction of new container yards, and the improvement of ground conditions in an area reserved for future yard expansion. Some of the main characteristics of the project and its construction method, along with a description of the soil profile can be found elsewhere (Larrague and Sfriso, 2001).

A 80000 m², 3.5 m high preload embankment (PE) was put on top of the permanent fill for ground improvement purposes. Because of operational requirements of the terminal, the PE construction was delayed in a 6000 m² area, just beside of the existing yards and wharf, as shown in Figure 1.

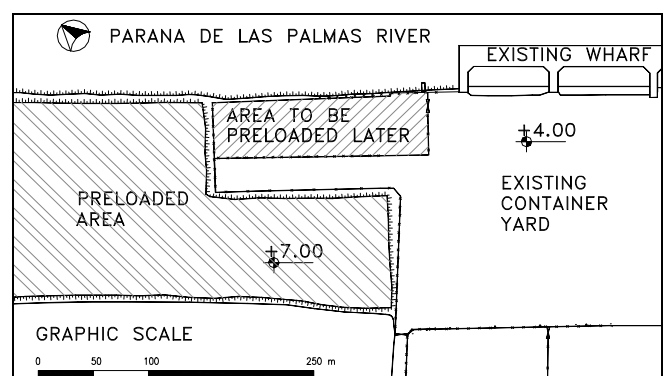


Figure 1. Plan sketch of the project.

Figure 2 shows a view of the preloaded area as it could be seen from the existing wharf. The embankment area not preloaded at the first stage is at the center of the picture.



Figure 2. Preload embankment as seen from the wharf.

Figure 3 shows a typical boring log, obtained after completion of the permanent fill and before placement of the preload embankment.

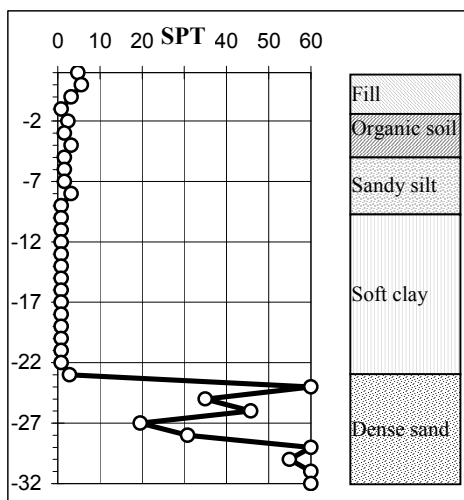


Figure 3. Boring log and soil profile.

As reported in a previous paper (Larrague and Sfriso, 2001), PE was placed in 120 days, and a consolidation degree of about 80% was achieved within three months. Settlement is approx. 1.20 m by the end of 2002, fairly consistent with the initial forecasts.

2 EMBANKMENT COLLAPSE

2.1 Placement of the preload embankment in a small area

Several months after the main PE completion and without any communication to the design engineers, the 6000 m² area located in the coastline and reserved for operational use was filled and preloaded within ten days.

2.2 Slope failure

One day after the completion of this PE, a massive slope failure occurred. Within a few seconds a 100 m by 40 m surface settled more than 2.50 m. The recently placed preload

material, as well as the underlying permanent fill, fell into the river. The whole sliding area was flooded.

Great concern about the stability of the remaining embankments arose in both the contractor's and owner's staffs, as it was apparent that a low river tide would induce progressive failure of larger areas of the embankment. Project engineers were immediately called in.

Figure 4 shows the sliding mass as seen from the wharf. The large inclination of the previously horizontal, flat surface is easily noticeable at the central left part of the picture. Fortunately, no people, equipment or any other facilities were at or near the sliding area.



Figure 4. Sliding mass as seen from the wharf.

Figure 5 is another view from the same place, showing that the coastline vegetation moved some 20 m into the river. One of the authors is there for scaling reference.



Figure 5. Coastline vegetation shifted 20 m into the river.

Many tension cracks could be observed both in the asphalt pavement of the old embankment and on top of the PE and recent permanent fill that remained. Cracks near the river immediately were filled with water, while cracks located at greater distances from the coastline remained open and dry.

2.3 Contingency action

A construction team, supervised by the project engineers, immediately started works to prevent subsequent damage. The following contingency actions were performed:

- Remaining soils from the PE were removed the same day of the slope failure.
- The embankment surface immediately behind the failure area was reshaped, and a 1:1 slope surface was cut and sealed.
- Tension cracks behind the sliding mass were excavated and back filled with soil.
- The failure surface was trimmed and reshaped manually. Cracks within the failed area were carefully filled with sand and soil and sealed at surface.

After the first remedial actions were performed, project engineers started a survey and investigation program to determine the causes of the failure and to design proper remedial actions.

3 ANALYSIS OF THE FAILURE

3.1 Preliminary analysis

A topographic survey was conducted to evaluate the magnitude and depth of the failed soil mass. At the same time, some preliminary stability computations were performed, because there was an immediate need of a reliable undrained shear strength value of the soils at the assumed sliding surface. Figure 6 shows the sketch of the plan view and the failure area.

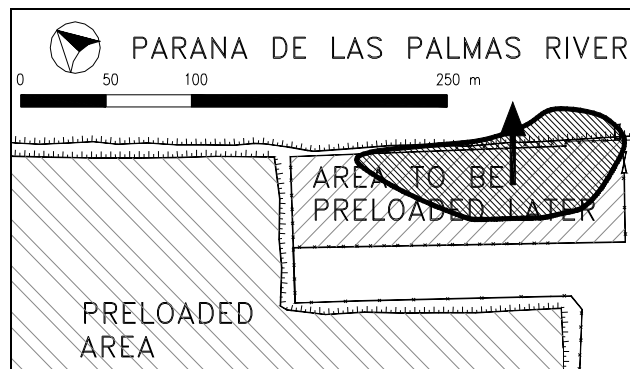


Figure 6. Sketch with sliding mass shown.

There was immediate agreement among the design engineers that the most probable cause of failure was a too high construction speed, because it was already known that the coastline slope was not stable under a fully undrained fill+PE surcharge. Water had been at its mean level the days before the failure occurred, so this particular source of soil overstressing was disregarded.

Therefore, the remediation program was limited to a slow placement of the fill after

compaction of the remaining materials, and a simple monitoring program to be maintained during the earthworks. No further inconveniences happened, and the embankment was completely repaired and, eventually, preloaded to the design height.

3.2 FE Back analysis of the failure

This unfortunate incident proved to be an excellent opportunity to learn from failure, as there was enough information about the soil conditions to perform a back analysis of the slope failure.

The analysis tool chosen was a 2D finite element model implemented in Plaxis, mainly because there was a need to simulate the different construction stages with varying drainage conditions.

Topographic and bathymetric surveys showed that failure had occurred at the bottom of the organic soil that lies on the sandy silt deposit. The height of the preload and the shape of the slope at failure were known, and therefore the key parameters for this problem were effective cohesion, effective friction angle and permeability of the organic soil layer. Parameters had to be found to yield superficial slope failure for a fully undrained analysis and no failure for an analysis that takes into account a three month construction period.

3.2.1 Soil characterization

Soils were characterized via the hyperbolic hardening plasticity model available in Plaxis (Brinkgreve and Vermeer, 1998) that follows the well-known hyperbolic model by Duncan and Chang (Duncan and Chang, 1970).

Table 1 lists the input parameters for the selected soil model. Most of these parameters were chosen after past experience and available correlations, some of which were published elsewhere (Sfriso, 1997; Sfriso, 1999, Larrague and Sfriso, 2001). Stiffness depends on mean pressure through a modification of a power law (Janbu, 1963)

$$E = E^{ref} \left(\frac{p}{100 \text{ KPa}} \right)^m$$

where E is Young modulus, E^{ref} is a reference value, p is mean pressure and m is an exponent. An effective cohesion linearly increasing with depth, assumed to exist in the deep clay deposit, can be modelled through

$$c = c + c_{incr} (y - y^{ref})$$

where y is depth, relative to reference level y^{ref} .

Table 1. Soil parameters of the five layers.

Identification	Level m	γ kN/m ³	k m/day	E_{50}^{ref} MPa	E_{oed}^{ref} MPa	E_{ur}^{ref} MPa	c KPa	ϕ °	ψ °	ν	m	K_0^{nc}	OCR	K_0	c_{incr} kN/m ³	y^{ref} m	R_f
Preload mat.	+7.0	19	2E-01	9.0	12.0	27.0	5	29	0	0.2	0.5	0.52	1.5	0.70	-	-	0.9
Permanent fill	+4.0	19	1E+00	10.0	12.0	30.0	12	30	2	0.2	0.5	0.56	4.0	0.80	-	-	0.9
Organic soil	+1.0	15	?	0.9	0.9	3.3	?	?	0	0.2	1.0	0.56	1.5	0.72	-	-	0.8
Sandy silt	-1.0	18	1E-01	5.0	5.0	15.0	1	28	0	0.2	0.8	0.53	1.5	0.67	-	-	0.9
Plastic clay	-6.0	16	1E-04	1.1	1.0	3.3	1	24	0	0.2	1.0	0.59	1.2	0.66	0.10	20	0.8

In the previous table, γ is total unit weight, k is estimated mean field permeability, E_{50}^{ref} is elastoplastic reference stiffness at 50% shear mobilization, E_{oed}^{ref} is oedometric reference stiffness, E_{ur}^{ref} is unload-reload elastic reference stiffness, c is effective cohesion, ϕ is effective stress friction angle, ψ is dilatancy angle, ν is Poisson ratio, m is Jambu coefficient, K_0^{nc} is at rest pressure coefficient at normally consolidated soil conditions, K_0 is at rest pressure coefficient at actual OCR, c_{incr} is the increment of effective cohesion with depth, y^{ref} is the reference level for computation of c_{incr} , and R_f is Duncan-Chang shear ratio at failure.

3.2.2 Mesh and construction stages

A FE mesh with 938, fifteen node triangular elements was used. Figure 7 shows the construction stages considered.

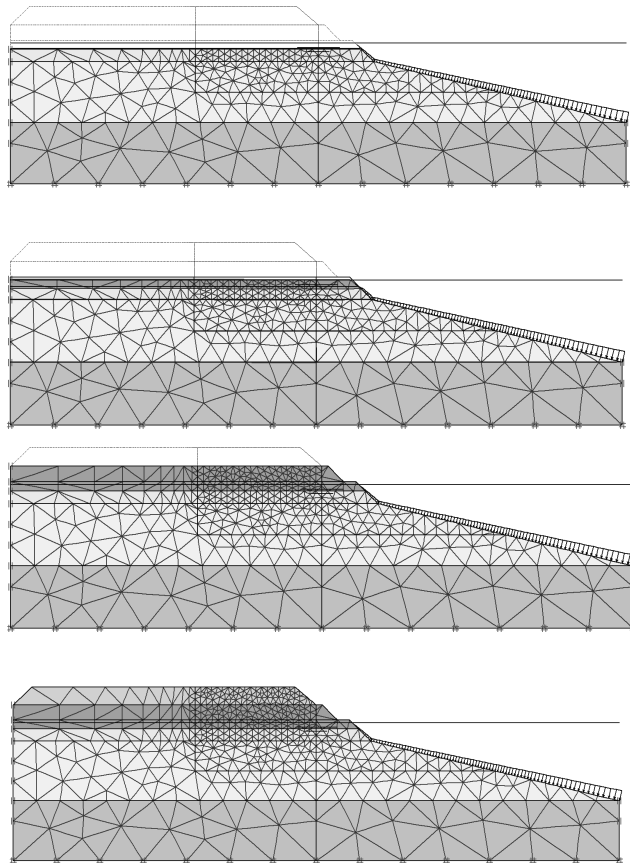


Figure 7. Mesh and construction stages.

The first construction stage is the natural shoreline, so no pore pressure build up was allowed there. Second stage is the placement of the first two meters of compacted fill, which happened long time before this project started, and was also modeled as a drained stage. Third stage is the placement of the permanent fill and the fourth stage is the placement of the preload embankment.

Two separate analysis were performed:

- 1 A fully undrained analysis, simulating the behaviour of the small embankment that failed.
- 2 A stepped undrained – consolidation analysis, where each construction stage was followed by a consolidation stage equivalent to a 30 day lag in construction time, thus simulating the real construction schedule.

3.2.3 Results

After some trial and error, the final strength and permeability parameters that best matched the observed behaviour of the embankment were

$$c = 1 \text{ KPa}$$

$$\phi = 26^\circ$$

$$k = 0.085 \text{ m/day}$$

Cohesion is assumed to be zero, but a small value is accepted to improve numerical performance. The computed effective friction angle is somewhat lower than the forecasted value. Triaxial tests of these organic soils, performed on vertical samples, yielded friction angles in the range 28° - 32°.

The partially consolidated model yielded no failure, whereas the fully undrained model failed at about 40%-60% of the full preload stage.

Onset of failure was not a slope stability problem but the squeeze of a very soft plastic layer, as shown in Figure 8, where only strain increments above mean value were plotted. This plot shows which portions of the model are increasing their velocity without control, and thus suggests where failure starts from.

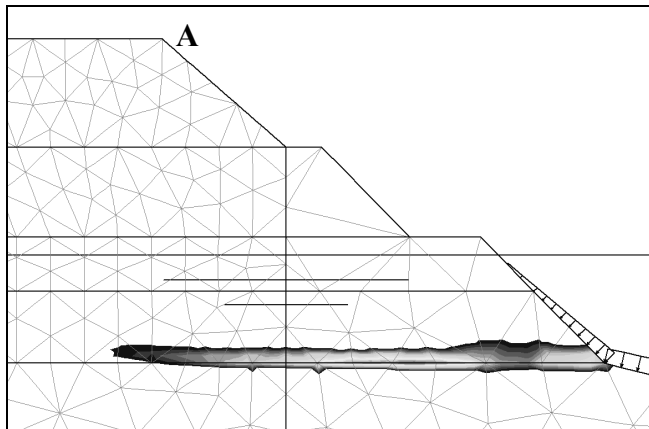


Figure 8. Strain increments at the onset of failure. Undrained analysis.

Figure 9 shows the deformed mesh of the second model. A 1.20 m max. settlement was achieved but movements eventually ceased, in a similar performance to that of reality.

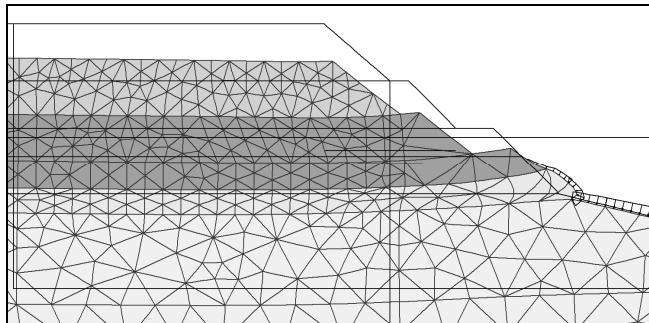


Figure 9. Settlements in partially drained analysis. Máx settlement is 1.25 m.

Figure 10 shows the displacement of the edge of the preload embankment, marked as “A” in Figure 8. It can be seen that total settlement for the partially drained model is 1.20 m, and that it’s behaviour is stable, whereas the undrained analysis began to fail at about 40% of the full PE load.

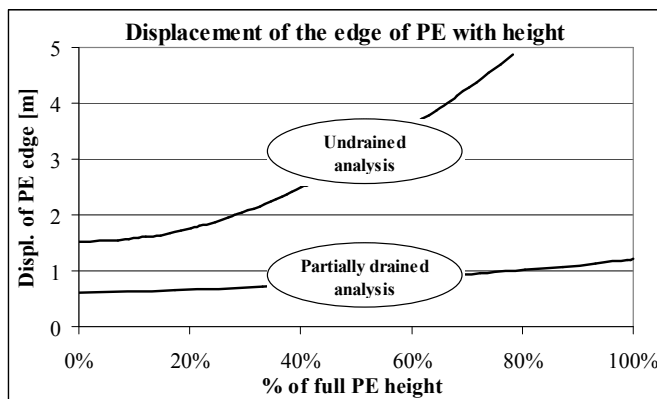


Figure 10. Displacement of the edge of PE during placement of the preload.

4 CONCLUSIONS

An embankment and ground improvement program was designed to speed up the construction process of a container yard. This program proved successful, as the construction time was cut off by a factor of three (Larrague and Sfriso, 2001). A small portion of the job remained uncompleted due to an owner’s decision. Some months later, the contractor completed the job by himself. Too high a construction speed triggered a slope failure.

In this paper, a back analysis of this failure was presented. It was shown that the slope failure started with the displacement of a thin, weak layer of organic soils that squeezed out of the toe embankment.

The full process of construction, load and consolidation was modeled twice: as a simulation of rapid construction in a fully undrained analysis, and at real speed construction in a staged load-consolidation scheme. These two models were calibrated with the same input parameters, yielding a back-analysis value of effective friction angle and field permeability of the organic soil layer. This procedure is not intended to find “true” values for these soil parameters, but to calibrate the available constitutive models for local soils.

The combination of judgement, numerical analysis and interpretation of field data allowed for a safe completion of the project without further inconveniences. Figure 11 shows an aerial view of the wharf and yard today. A dotted arc shows the place where slope failure occurred, with some containers on it.



Figure 11. Aerial view of the site after rehabilitation works.

5 ACKNOWLEDGEMENTS

The authors want to acknowledge University of Buenos Aires, where they lecture, Murchison SA, for the permission to publish the data, and Prof. Eduardo Núñez, for his permanent guidance and support.

6 REFERENCES

- Brinkgreve, R. and P. Vermeer (1998). *Plaxis manual*. Balkema, 425 p.
- Duncan, J. and C. Chang (1970) "Nonlinear analysis of stress and strain in soils" Journal of Soil Mechanics Foundation Division, ASCE, 96, SM5, 1629-1653.
- Janbu, N. (1963). "Soil compressibility as determined by oedometer and triaxial tests". Proc. Eur. Conf. Soil Mech. Found. Eng., Wiesbaden, I, 19-25.
- Larrague, J. y A. Sfriso. (2001). "Ground improvement in Zárate". In: Foundations and Ground Improvement, Geo. Sp. Pub 113, ASCE, 514-523.
- Núñez, E. (1994). "Propiedades mecánicas de materiales granulares incoherentes". In: Anales Acad. Nac. Cs. Ex. Fís. Nat., Buenos Aires, 46, 71-89.
- Núñez, E (1997) "Interacción suelo – estructura: Predicción, Comportamiento e instrumentación de campo". In: 1st Congreso Paraguayo de Ingeniería Geotécnica, Asunción, 1-19.
- Sfriso, A. (1997). "Formación Postpampeano. Predicción de su comportamiento mecánico". In: 3rd CLIGJ, Caracas, pp. 1-10.
- Sfriso, A. (1999). "Tunnels in Buenos Aires: Application of numerical methods to the structural design of linings". In: XI Panamerican Conference on soil mechanics and geotechnical engineering. 637-642.